

# Influence of strain on microwave dielectric properties of (Ba,Sr)TiO<sub>3</sub> thin films

Wontae Chang<sup>a)</sup> and Charles M. Gilmore

*Institute for Material Science, School of Engineering Applied Science, George Washington University, Washington, DC 20052*

Won-Jeong Kim

*SFA Inc., 1401 McCormick Drive, Largo MD 20744*

Jeffrey M. Pond, Steven W. Kirchoefer, Syed B. Qadri, Douglas B. Chirsey and James S. Horwitz<sup>b)</sup>

*Naval Research Laboratory, 4555 Overlook Avenue SW, Washington, DC 20375*

(Received 30 September 1999; accepted for publication 15 December 1999)

Epitaxial Ba<sub>1-x</sub>Sr<sub>x</sub>TiO<sub>3</sub> (BST) thin films have been deposited onto (100)MgO and LaAlO<sub>3</sub> substrates using pulsed-laser deposition. Thick (>1 μm) Ag interdigitated capacitors capped with a thin protective layer of Au have been deposited on top of the BST films using electron-beam deposition. The capacitance (*C*) and dielectric quality factor ( $Q = 1/\tan \delta$ ) of the structure has been measured at microwave frequencies (1–20 GHz) as a function of electric field ( $E \leq 67$  kV/cm) at room temperature. In epitaxial BST films, either high dielectric tuning (4:1), which is defined as  $\{[C(0) - C(E)]/C(0)\} \times 100$ , or high dielectric *Q* (~100–250) was observed but not both at the same time. Film strain was observed by x-ray diffraction and is closely related to the dielectric properties as limiting the ability to obtain both high tuning and high dielectric *Q* in epitaxial BST thin films. A thin BST buffer layer was used to relieve the strain in the films. In strain-relieved films, both dielectric tuning and dielectric *Q* were increased after annealing. A theoretical analysis of the strain effect of the films is presented based on Devonshire thermodynamic theory. © 2000 American Institute of Physics. [S0021-8979(00)08206-2]

## I. INTRODUCTION

Ba<sub>1-x</sub>Sr<sub>x</sub>TiO<sub>3</sub> (BST) is a solid-solution ferroelectric material that exhibits an electric-field-dependent dielectric constant and (Ba,Sr) composition-dependent Curie temperature.<sup>1</sup> These properties are currently being used to develop high-frequency (1–20 GHz) tunable microwave devices for room-temperature application. One of the most critical properties that needs to be maximized for this application is the dielectric *Q* of ferroelectric materials at high frequencies (>2 GHz).

Stress is a very significant factor affecting the dielectric properties. It has been reported that hydrostatic compression or two-dimensional compression parallel to the electrode of a parallel capacitor filled in a bulk ferroelectric leads to a decrease in the dielectric constant and the Curie temperature (*T<sub>C</sub>*).<sup>2–4</sup> The application of two-dimensional compression normal to the electrode was also reported to induce an increase in the dielectric constant and *T<sub>C</sub>*.<sup>5,6</sup> The effects of the stress on the dielectric constant and the *T<sub>C</sub>* are due to the fact that ionic positions and vibrations in a ferroelectric are modified by the stress, and these changes are coupled to the polarization mechanism in the ferroelectric.

In this article, we report an investigation of the effects of film strain on the dielectric properties (1–20 GHz) of epitaxial BST (*x*=0.5) films deposited by pulsed-laser deposition

(PLD). Film stress in heteroepitaxial films can be caused by the mismatch between the lattice parameters and thermal expansion coefficients of the film and substrate. A systematic survey of the dielectric properties of the PLD-grown film and a theoretical analysis of the observed data are presented.

## II. EXPERIMENT

BST (*x*=0.5) thin films (~0.5 μm thick) were grown on (100)MgO and LaAlO<sub>3</sub> (LAO) single-crystal substrates at 750 °C in an oxygen ambient pressure of 350 mTorr by pulsed-laser deposition. The PLD system used to grow the BST films has been described previously.<sup>7</sup> The output of a short-pulsed (30 ns full width at half maximum) excimer laser operating with KrF (λ=248 nm) at 5 Hz was focused to a spot size of ~0.1 cm<sup>2</sup> and an energy density of ~1.9 J/cm<sup>2</sup> onto a single-phase BST (*x*=0.5) target. The vaporized material was deposited onto a heated substrate approximately 4 cm away from the target. The target was a 2 in. diam by 0.125 in. thick sintered disk (Ba<sub>0.5</sub>Sr<sub>0.5</sub>TiO<sub>3</sub>, Target Materials Inc.). BST films were also deposited using a two-step procedure. First, a thin (~50 Å) amorphous BST buffer layer was deposited at room temperature. The substrate temperature was then increased to 750 °C and a second BST film (~0.5 μm thick) was deposited. Films deposited by both procedures were characterized for structure and morphology using x-ray diffraction (XRD) and scanning electron microscopy (SEM). Films were annealed in flowing O<sub>2</sub> at 900–1250 °C for 6–24 h. In-plane and normal lattice parameters

<sup>a)</sup>Electronic mail: chang@ccf.nrl.navy.mil

<sup>b)</sup>Electronic mail: horwitz@ccsalpha3.nrl.navy.mil

TABLE I. Average and maximum values of the dielectric constant and dielectric  $Q$  for annealed BST films (1–20 GHz) as a function of substrate type ( $\epsilon$ =film dielectric constant, % dielectric tuning at  $E=67$  kV/cm, and dielectric  $Q$ ).

Substrate	Average		Maximum data			
	MgO	LAO	MgO	LAO	MgO	LAO
$\epsilon$	1000	1500	2973	763	3328	1003
% tuning	30	50	62	22	75	9
$Q$	45	25	5–20	100–250	4–44	50–70

of the films were measured using XRD as a function of substrate type and annealing temperature. Interdigitated capacitors with gaps from 5 to 12  $\mu\text{m}$  were deposited on top of the BST films through a polymethylmethacrylate (PMMA) lift-off mask by e-beam evaporation of 1–2- $\mu\text{m}$ -thick Ag and a protective thin layer of Au.<sup>8</sup>

Microwave input reflection coefficient  $S_{11}$  measurements were made on an HP 8510C network analyzer at room temperature. The data are fitted to a parallel resistor–capacitor model to determine capacitance and dielectric  $Q$ .<sup>8</sup> Dielectric constants were calculated from the device dimensions.

### III. RESULTS AND DISCUSSION

#### A. Film strain and microwave dielectric properties

Previously, we reported on the annealing effect on the microwave (1–20 GHz) dielectric properties of epitaxial BST films deposited on MgO and LAO substrates.<sup>9</sup> It was observed that for the films deposited onto MgO, the dielectric constant decreased and dielectric  $Q$  increased after a postdeposition anneal ( $\leq 1000^\circ\text{C}$ ).<sup>9</sup> However, for films deposited onto LAO, the postdeposition anneal resulted in a significant increase in the dielectric constant and a decrease in  $Q$ .<sup>9</sup> Table I shows the general trends and maximum data of dielectric properties for the BST ( $x=0.5$ ) films at 1–20 GHz as a function of substrate type. In epitaxial BST films, we typically observed either a large dielectric tuning (75%) or a high dielectric  $Q$  (100–250) but not both at the same time. It was suggested that the differences in the dielectric properties of epitaxial BST films on MgO and LAO are due to differences in film strain.<sup>9</sup>

To determine the film strain, we measured the lattice parameters of epitaxial BST ( $x=0.5$ ) films deposited at a substrate temperature of  $750^\circ\text{C}$  and  $\text{O}_2$  pressure of 350 mTorr. The lattice parameters along the surface normal ( $a_\perp$ ) and in the plane of the films ( $a_\parallel$ ) were determined from XRD patterns of (004) and (024) reflections for (001)-oriented BST films.<sup>10,11</sup> The structure of the thin film was measured as a function of substrate type (MgO and LAO), the temperature of a postdeposition anneal (900–1250  $^\circ\text{C}$  for 6 h), and film thickness ( $\sim 500$ –2000  $\text{\AA}$ ).<sup>10,11</sup> In these studies, four important observations were made. First, both normal and in-plane lattice parameters of the films were 0.1%–0.3% and 0.2%–0.8% greater than the lattice parameter ( $a = 3.947$   $\text{\AA}$ ) of the corresponding bulk BST ( $x=0.5$ ) material, respectively. Second, the in-plane lattice parameter of the films was 0.1%–0.7% larger than the normal lattice pa-

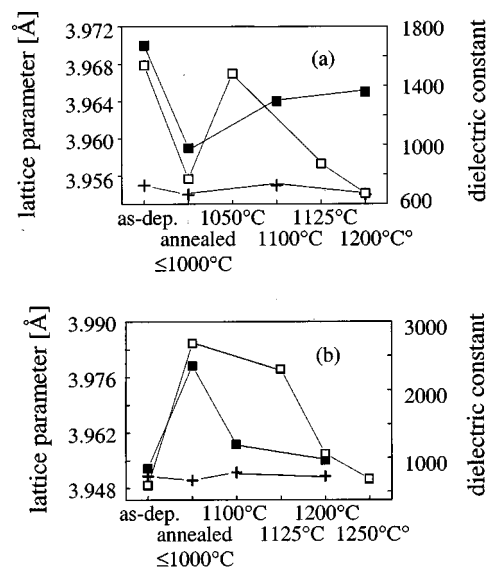


FIG. 1. Lattice parameter and dielectric constant changes with annealing temperature for BST ( $x=0.5$ ) films deposited onto (a) MgO and (b) LAO ( $\text{+}$ =normal lattice parameter,  $\blacksquare$ =in-plane lattice parameter, and  $\square$ =dielectric constant).

rameter, resulting in an in-plane tetragonal lattice distortion ( $a_\parallel > a_\perp$ ), although the structure for the corresponding bulk is a cubic. Third, after annealing ( $\leq 1000^\circ\text{C}$ ), the in-plane lattice parameter decreased for films deposited onto MgO and the opposite effect was observed for films deposited onto LAO. Fourth, the measured in-plane lattice parameters were closely correlated with the observed dielectric constant, as shown in Fig. 1. These observations are very important to our understanding of how to control the dielectric properties of the film. The observations of the lattice distortion and lattice expansion are due to lattice mismatch and thermal coefficient mismatch between film and substrate and oxygen vacancies in the film.

To calculate the film strain, we have to know the equilibrium lattice parameter  $a_0$  of the film, which is different from the corresponding bulk lattice parameter for several reasons, such as oxygen vacancies in the film and interactions between the film and substrate. Therefore, the equilibrium lattice parameter (3.947  $\text{\AA}$ ) of bulk BST ( $x=0.5$ ) cannot be used for strain calculations of the film. Generally, it is difficult to know the equilibrium lattice parameter of the film without detailed information of the oxygen vacancies in the film. Alternatively, the equilibrium lattice parameter of PLD BST ( $x=0.5$ ) film deposited at  $\text{O}_2$  pressure of 350 mTorr was estimated from XRD measurement for the BST ( $x=0.5$ ) film deposited with a thin amorphous BST buffer layer. The amorphous BST buffer layer was used to remove the strain in the subsequently deposited crystalline BST film caused by the mismatch between the lattice constants and thermal expansion coefficients of the epitaxial film and the substrate. BST films deposited with the BST buffer layer are single phase but not a single-crystallographic orientation as determined by XRD. The intensities of the XRD peaks are similar to the corresponding powder diffraction pattern. The estimated equilibrium lattice parameter for a BST ( $x=0.5$ ) film was 3.961  $\text{\AA}$ , which was very close to the lattice param-

TABLE II. Film strain and dielectric constant of epitaxial BST ( $x=0.5$ ) films deposited onto (100)MgO and (100)LAO at a substrate temperature of 750 °C and O<sub>2</sub> pressure of 350 mTorr.

	BST onto (100)MgO		BST onto (100)LAO	
	As-deposited	Annealed $\leq 1000$ °C	As-deposited	Annealed $\leq 1000$ °C
$a_{\parallel}$ [Å]	3.970	3.959	3.953	3.978
$a_{\perp}$ [Å]	3.955	3.954	3.951	3.950
$a_0$ (Å) using a buffer layer			3.961	
$a_0$ (Å) using Eq. (1) <sup>a</sup>		3.959		3.958
Estimated in-plane strain (%)	0.23	-0.05	-0.20	0.42
Based XRD measurement				
Measured dielectric constant	1540	770	875	2500
Estimated in-plane strain (%)	0.033	-0.031	-0.023	0.064
Based on theory				

<sup>a</sup>References 12 and 13.

eters estimated from the normal lattice parameter  $a_{\perp}$  and the in-plane lattice parameter  $a_{\parallel}$  measured by XRD using the following equation as presented in Table II:<sup>12,13</sup>

$$a_0 = \{a_{\perp} - (x_3/x_1)a_{\parallel}\} / \{1 - (x_3/x_1)\}, \quad (1)$$

where  $x_3$  and  $x_1$  are the strain along the surface normal and in the plane of the films and  $x_3/x_1$  can be related through the elastic constants  $c_{ij}$  of the film;  $x_3/x_1 = -2(c_{12}/c_{11})$  for equiaxial strain from the substrate ( $x_1 = x_2$ ). With the estimated equilibrium lattice parameter for the thin film (3.961 Å), we can show that the as-deposited films on MgO substrates are in tension parallel to the film surface and the annealed ( $\leq 1000$  °C) films are in compression, and the opposite effect for films deposited onto LAO. The strain in the in-plane film is closely related to the change of the dielectric constants for our experimental configuration, as shown in Table III. The experimentally observed relationship between the film strain and the dielectric constant can be interpreted using Devonshire's thermodynamic theory.

## B. Theoretical analysis of the dielectric properties of epitaxial BST films

Devonshire developed a phenomenological theory to explain the ferroelectric behavior of bulk BaTiO<sub>3</sub>.<sup>14-16</sup> According to the theory, the Gibbs free energy ( $G$ ) of a stress-free ferroelectric subject to external electric fields ( $E$ ) can be expressed as

$$G(T, P_i) = F(T, P_i) - E_i P_i, \quad (2)$$

where  $F$  and  $P_i$ , are the Helmholtz free energy ( $F$ ) of a strain-free ferroelectric and polarization, respectively. When the ferroelectric is subjected to stresses ( $X$ ), the Helmholtz free energy should also expanded with strains ( $x$ ) as follows:

$$\begin{aligned} F(T, P_i, x_j) &= F_0 + 1/2\alpha(P_1^2 + P_2^2 + P_3^2) + 1/4\beta(P_1^4 + P_2^4 + P_3^4) \\ &+ 1/6\gamma(P_1^6 + P_2^6 + P_3^6) \\ &+ 1/2\delta(P_2^2 P_3^2 + P_3^2 P_1^2 + P_1^2 P_2^2) \\ &+ 1/2c_{11}(x_1^2 + x_2^2 + x_3^2) + c_{12}(x_2 x_3 + x_3 x_1 + x_1 x_2) \end{aligned}$$

$$\begin{aligned} &+ 1/2c_{44}(x_1^2 + x_2^2 + x_3^2) \\ &+ G_{11}(x_1 P_1^2 + x_2 P_2^2 + x_3 P_3^2) + G_{12}\{x_1(P_2^2 + P_3^2) \\ &+ x_2(P_3^2 + P_1^2) \\ &+ x_3(P_1^2 + P_2^2)\} + G_{44}(x_4 P_2 P_3 + x_3 P_3 P_1 + x_6 P_1 P_2) \\ &+ \dots, \end{aligned} \quad (3)$$

where  $F_0$  is a function of temperature alone,  $F_0 = (T, 0, 0)$ ,  $\alpha$ ,  $\beta$ ,  $\gamma$ , and  $\delta$  are the free-energy expansion coefficients, and  $c_{ij}$  and  $G_{ij}$  are the elastic constants and the stress-polarization-related electrostrictive coefficients, respectively. Assuming that for epitaxial films (1) the equibiaxial in-plane strains  $x_1$  and  $x_2$  are controlled by the substrate, (2)  $X_3$  is zero on the free surface of the film, (3) in-plane polarization occurs only in one direction for the interdigitated capacitor as the simplest case, and (4) the electric fields are parallel to the polarization, the Gibbs free energy becomes

$$\begin{aligned} G(T, P, X_j) &= F(T, P, x_j) - EP \\ &= F_0 + 1/2\alpha P^2 + 1/4\beta P^4 + 1/6\gamma P^6 \\ &+ 1/2c_{11}(x_1^2 + x_2^2 + x_3^2) + c_{12}(x_2 x_3 + x_3 x_1 \\ &+ x_1 x_2) + 1/2c_{44}(x_1^2 + x_2^2 + x_3^2) + G_{11}x_1 P^2 \\ &+ G_{12}(x_2 + x_3)P^2 - EP. \end{aligned} \quad (4)$$

Since the Gibbs free energy  $G$  must be a minimum for a stable state of the ferroelectric at a constant temperature ( $\partial G/\partial P = 0$ ), we have the following relationship:

$$\begin{aligned} \partial F/\partial P - E &= \alpha P + \beta P^3 + \gamma P^5 \\ &+ 2G_{11}x_1 P + 2G_{12}(x_2 + x_3)P - E = 0. \end{aligned} \quad (5)$$

We can neglect the contribution from the fifth-order or greater terms in  $P$ .<sup>17</sup> Also, we can assume  $P = \epsilon E$  in the case of small electric fields  $E$  or in the case of relatively large electric fields for a paraelectric state of a ferroelectric. Then, we have the following relationship between the dielectric constant and the applied electric field by differentiating Eq. (5) with respect to  $P$ :

$$\partial E/\partial P = \alpha + 3\beta(\epsilon E)^2 + 2G_{11}x_1 + 2G_{12}(x_2 + x_3) = 1/\epsilon. \quad (6)$$

The first-order coefficient  $\alpha$  of the expansion of the applied electric field  $E$  with polarization  $P$  should be  $1/\epsilon$  for strain-free materials. The coefficient  $\alpha$  for BST ( $x=0.5$ ) can be estimated from the Curie constants of bulk STO and BTO ferroelectrics. The stress-polarization-related electrostriction coefficients  $G_{11}$  and  $G_{12}$  can be obtained from the following equation:<sup>18</sup>

$$G_{ij} = c_{ik} Q_{kj} \quad (i, j, k = 1, \dots, 6), \quad (7)$$

where  $Q_{kj}$  are the strain-polarization-related electrostriction coefficients and  $c_{ik}$  and  $Q_{kj}$  can be obtained from the literature.<sup>19-23</sup> The expressions are written in a single-index matrix notation. For example, 1=11, 2=22, 3=33, 4=23, 5=31, and 6=12 where 1, 2, and 3 in the double-index notation can be  $x$ ,  $y$ , and  $z$  in the rectangular coordinate system. The relevant coefficients used in the theoretical calculations

TABLE III. Relevant coefficients used in the theoretical calculations of the dielectric properties of BST ( $x=0.5$ ) films deposited at a substrate temperature of 750 °C and O<sub>2</sub> pressure of 350 mTorr.

Description		Ref.	
$T_C$ (K)	Curie temp. for bulk BST ( $x=0.5$ )	250	19
$C_{STO}$ (10 <sup>5</sup> K)	Curie constant for bulk STO	0.8	20
$C_{BTO}$ (10 <sup>5</sup> K)	Curie constant for bulk BTO	1.5	21
$Q_{11}$ (m <sup>4</sup> /C <sup>2</sup> )	Electrostriction coefficient	-0.10	22
$Q_{12}$ (m <sup>4</sup> /C <sup>2</sup> )	Electrostriction coefficient	0.034	22
$c_{11}$ (10 <sup>11</sup> N/m <sup>2</sup> )	Elastic constant for bulk STO	3.4817	23
$c_{11}$ (10 <sup>11</sup> N/m <sup>2</sup> )	Elastic constant for bulk BTO	2.7512	23
$c_{12}$ (10 <sup>11</sup> N/m <sup>2</sup> )	Elastic constant for bulk STO	1.0064	23
$c_{12}$ (10 <sup>11</sup> N/m <sup>2</sup> )	Elastic constant for bulk BTO	1.7897	23

of the dielectric properties of BST ( $x=0.5$ ) films are presented in Table III. The theoretical dielectric constant at zero field of both strain-free and strained bulk BST ( $x=0.5$ ) can be calculated from Eq. (6). In Eq. (6), a change in the strain terms leads to a shift of  $T_C$  to lower temperatures or higher temperatures for compressive or tensile strain, respectively. However, in the case of tensile strain which causes a shift of  $T_C$  to higher temperatures so that the film is in a ferroelectric phase at  $T$ , Eq. (6) cannot be used. Instead, a relationship between film strain and dielectric constant in a ferroelectric phase can be obtained from Eq. (5). In a ferroelectric phase, the film must have only spontaneous polarization ( $P_S$ ) with a zero field ( $E=0$ ):

$$E = \alpha P_S + \beta P_S^3 + \gamma P_S^5 + 2G_{11}x_1 P_S + 2G_{12}(x_2 + x_3)P_S = 0. \tag{8}$$

By differentiating Eq. (5) with respect to  $P$  and then substituting the spontaneous polarization ( $P_S$ ) from Eq. (8), we obtain a relationship between the film strain and dielectric constant for a ferroelectric phase:

$$\left(\frac{\partial E}{\partial P}\right)_{P_S} = -2\alpha - 4G_{11}x_1 - 4G_{12}\{1 - 2(c_{12}/c_{11})\}x_1 = 1/\epsilon. \tag{9}$$

Figure 2 shows theoretical variations of the dielectric constant with strain for BST ( $x=0.5$ ) at room temperature. The dielectric constant increases rapidly with tension and decreases gradually with compression in a paraelectric phase. Assuming that the change in the dielectric constant with strain for both bulk and BST films shows a similar trend according to the literature reports on the strain effect on the dielectric constant,<sup>24,25</sup> the strain-dielectric constant dependence of the BST ( $x=0.5$ ) film was reproduced from that of bulk BST ( $x=0.5$ ) by setting the strain-free dielectric constant from 2300 for the bulk BST ( $x=0.5$ ) to 1020 for BST ( $x=0.5$ ) film. The strain-free dielectric constant for the BST ( $x=0.5$ ) film was obtained from the measurements with three BST films which were deposited with an amorphous BST buffer layer ( $\epsilon=1020\pm30$ ). Table III shows both experimentally estimated in-plane strain and theoretically estimated in-plane strain of epitaxial BST ( $x=0.5$ ) films deposited onto (100)MgO and (100)LAO at a substrate temperature of 750 °C and O<sub>2</sub> pressure of 350 mTorr. The latter was calculated using the measured dielectric constants

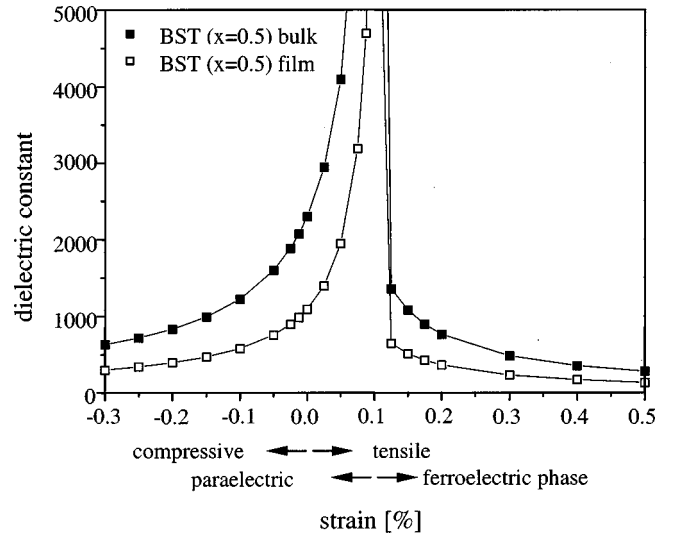


FIG. 2. Theoretical analysis of the strain-dielectric constant dependence for BST ( $x=0.5$ ) at room temperature.

of as-deposited and annealed ( $\leq 1000$  °C) BST ( $x=0.5$ ) films presented in Table II. Even though both estimations agree qualitatively in terms of the type of strain, i.e., compressive or tensile, they show one order of magnitude difference.

Strain in an epitaxial ferroelectric thin film can be caused by lattice parameter and thermal expansion mismatch between film and substrate, the volume changes associated with the ferroelectric phase transition, and compositional deficiencies such as Ba, Sr, and O vacancies. Among these strain-causing factors, the strain due to the phase transformation for BST ( $x=0.5$ ) may not be applicable in a room-temperature application because BST ( $x=0.5$ ) has no phase transition between the film processing temperatures and room temperature. Therefore, only strain due to the lattice mismatch  $x_l = (a_s - a_f)/a_f$  and thermal expansion mismatch  $x_t = (\alpha_s - \alpha_f)\Delta T$  are considered in how the strain is formed for as-deposited and annealed BST ( $x=0.5$ ) films. In the strain expressions of  $x_l$  and  $x_t$ ,  $a_s$  and  $a_f$  are the equilibrium lattice parameters, and  $\alpha_s$  and  $\alpha_f$  the thermal expansion coefficients of the substrate and film. Relevant coefficients were reported previously.<sup>9</sup> Both the estimated strain for as-deposited and annealed BST ( $x=0.5$ ) film, based on XRD measurements and theory, shown in Table III, are not consistent with the strain calculated directly from the lattice mismatch and thermal expansion mismatch. This difference may be due to oxygen vacancies and film relaxation effects such as the formation of misfit dislocations.<sup>26,27</sup> If we include the film relaxation into the strain term caused by the lattice mismatch, we can estimate the strain relief due to film relaxation. For example, by comparing the theoretically estimated strain (0.00033 and -0.00031 in Table III) to the calculated strain due to the lattice mismatch and thermal expansion mismatch ( $x_l + x_t$ ), the relieved strain is estimated as -0.059 and -0.062 for the as-deposited BST ( $x=0.5$ ) film and for annealed ( $\leq 1000$  °C) film onto (100)MgO, respectively. This estimation indicates that most (94%) of the strain due to lattice mismatch (+0.063) for the as-deposited film and 98%

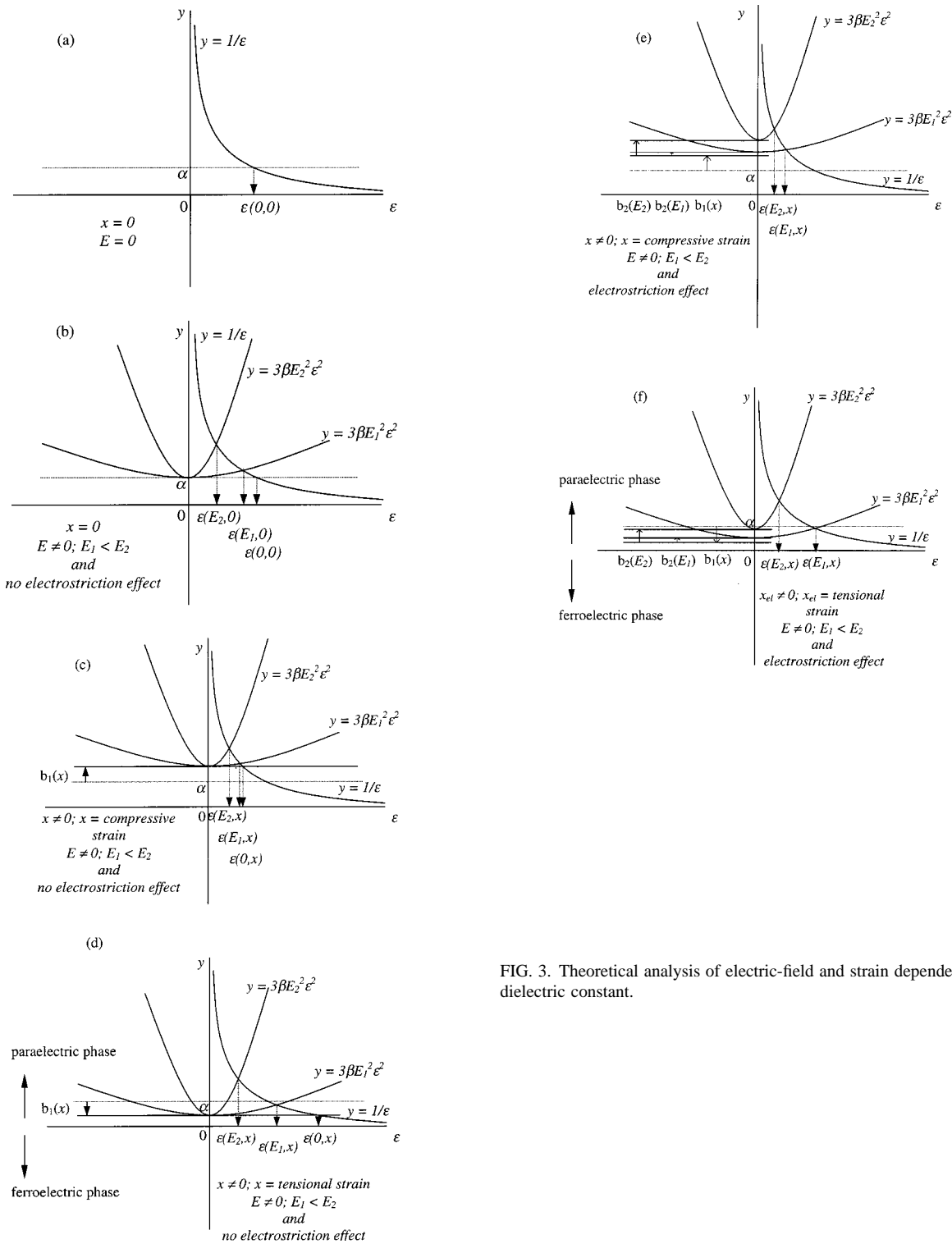


FIG. 3. Theoretical analysis of electric-field and strain dependencies of the dielectric constant.

of the strain due to the lattice mismatch for the annealed ( $\leq 1000^\circ\text{C}$ ) film are relieved by the film relaxation mechanism.

It is also important to understand the dielectric constant as a function of applied field in a strained ferroelectric. The electric-field dependence of the dielectric constant of the film can be analyzed theoretically from Eq. (6). When the electric field  $E$  is applied, the total strain can be expressed as

$$x_i = x_{el} + x_p + x_{es} = s_{ij}X_j + d_{ki}E_k + R_{ikl}E_kE_l$$

$$(i, j = 1, \dots, 6; k, l = 1, 2, 3), \tag{10}$$

where  $x_{el}$ ,  $x_p$ , and  $x_{es}$  are strains due to elasticity, piezoelectricity, and electrostriction, respectively,  $d$  is the piezoelectric coefficient, and  $R$  is the strain–electric-field-related electrostriction coefficients. Then, Eq. (6) becomes, without the piezoelectric effect for BST ( $x=0.5$ ) at room temperature,

$$\partial E / \partial P = 1/\epsilon = \alpha + 3\beta E^2 \epsilon^2 + b_1(x_{el}) + b_2(E), \tag{11}$$

where  $b_1(x_{el})$  is  $2G_{11}x_{el} + 2G_{12}\{1 - 2(c_{12}/c_{11})\}x_{el}$  and  $b_2(E)$  is  $2G_{11}R_{11}E^2 + 2G_{12}\{1 - 2(c_{12}/c_{11})\}R_{11}E^2$ . Then, we can plot the left side of Eq. (11),  $y = 1/\epsilon$ , and the right side,  $y = \alpha + 3\beta E^2 \epsilon^2 + b_1(x_{el}) + b_2(E)$ , to have a dielectric constant  $\epsilon(E, x)$  satisfied by both equations as a function of electric field and strain. To visualize the effect of strain and dc electric field on the dielectric constant, providing insight into how the dielectric tuning is performed depending on the strain, Eq. (11) is plotted in Fig. 3. The strain-free and zero electric-field dielectric constant  $\epsilon(0, 0)$  is presented in Fig. 3(a). When we apply dc electric fields  $E_1$  and  $E_2$  ( $E_2 > E_1$ ), the strain-free and nonzero electric-field dielectric constant  $\epsilon(E, 0)$  can be seen in Fig. 3(b), where the expansion coefficient  $\beta$  was observed to be a positive number for our BST films experimentally. We can see an important characteristic property of the dielectric constant on the application of dc electric fields in Fig. 3(b); the strain-free dielectric constant decreases with increasing electric field. Now, we can see how the dielectric constant and its tuning change with strain in Figs. 3(c) and 3(d) by comparing with Fig. 3(b), which is for a strain-free case. For compressive strains, we have a positive  $b_1(x)$  in Eq. (11) causing the dielectric constant and its tuning to be decreased [Fig. 3(c)] and for tensional strain, we have a negative  $b_1(x)$  in Eq. (11) causing the dielectric constant and its tuning to be increased [Fig. 3(d)]. This theoretical analysis agrees well with our experimental results.<sup>9</sup> As-deposited BST films on MgO and annealed ( $\leq 1000^\circ\text{C}$ ) BST films onto LAO were extended in the in-plane parameters resulting in a high dielectric constant and tuning, while annealed BST films onto MgO and as-deposited BST films onto LAO were compressed in the in-plane parameters causing a low dielectric constant and tuning. Figures 3(b), 3(c), and 3(d) do not include the electrostriction effect even though the electric fields are applied for simplicity. However, the electrostriction effect should be included whenever the field is applied. Figures 3(e) and 3(f) show how the electrostriction effect reduces the dielectric constant. The lowering dielectric constant by the electrostriction effect is because  $b_2(E)$  is always positive in Eq. (11).

From this experimental and theoretical analysis, we conclude that the strain in the epitaxial films limits the ability to get both high tuning and high dielectric  $Q$  at the same time. A thin amorphous BST buffer layer was used to remove the strain in the films, improving the dielectric properties for tunable microwave applications. After annealing BST films with the buffer layer, we observed a very large grain size ( $d \sim 5000 \text{ \AA}$ ) for the films compared to other annealed films deposited at  $750^\circ\text{C}$  without the BST buffer layer ( $d \sim 1000\text{--}3000 \text{ \AA}$ ). In strain-relieved BST films, we observed that both dielectric tuning and dielectric  $Q$  were increased after annealing.

#### IV. SUMMARY

The dielectric properties of pulsed-laser deposited  $\text{Ba}_{1-x}\text{Sr}_x\text{TiO}_3$  ( $x=0.5$ ) ferroelectric films were measured at microwave frequencies (1–20 GHz) and analyzed theoretically as a function of electric field and strain based on Devonshire's thermodynamic theory. This model can be used to predict qualitatively the changes in the dielectric constant of the films as a function of temperature, electric field, and strain [ $\epsilon = \epsilon(T, E, x)$ ]. Film strain has a significant effect on both microstructure and dielectric properties of the film. A thin amorphous buffer layer was observed to reduce the film strain effectively. A further study on the buffer layer as a function of temperature and thickness is needed to optimize its effect.

#### ACKNOWLEDGMENTS

This work was supported by the Office of Naval Research and the NRL SPAWAR program.

- <sup>1</sup>L. Davis and L. G. Rubin, J. Appl. Phys. **24**, 1194 (1953).
- <sup>2</sup>W. J. Merz, Phys. Rev. **77**, 52 (1950).
- <sup>3</sup>J. C. Slater, Phys. Rev. **78**, 748 (1950).
- <sup>4</sup>R. F. Brown, Can. J. Phys. **39**, 741 (1961).
- <sup>5</sup>P. W. Forsbergh, Jr., Phys. Rev. **93**, 686 (1954).
- <sup>6</sup>W. R. Buessem, L. E. Cross, and A. K. Goswami, J. Am. Ceram. Soc. **49**, 36 (1966).
- <sup>7</sup>K. S. Grabowski, J. S. Horwitz, and D. B. Chrisey, Ferroelectrics **116**, 19 (1991).
- <sup>8</sup>S. W. Kirchoefer, J. M. Pond, A. C. Carter, W. Chang, K. K. Agarwal, J. S. Horwitz, and D. B. Chrisey, Microwave Opt. Technol. Lett. **18**, 168 (1998).
- <sup>9</sup>W. Chang, J. S. Horwitz, A. C. Carter, J. M. Pond, S. W. Kirchoefer, C. M. Gilmore, and D. B. Chrisey, Appl. Phys. Lett. **74**, 1033 (1999).
- <sup>10</sup>W. Chang, J. S. Horwitz, W. J. Kim, J. M. Pond, S. W. Kirchoefer, C. M. Gilmore, and D. B. Chrisey, Mater. Res. Soc. Symp. Proc. **541**, 693 (1999).
- <sup>11</sup>W. J. Kim, W. Chang, S. B. Qadri, J. S. Horwitz, and D. B. Chrisey, Mater. Res. Soc. Symp. Proc. **541**, 705 (1999).
- <sup>12</sup>G. Wagner, Cryst. Res. Technol. **33**, 681 (1998).
- <sup>13</sup>A. Segmüller, J. Vac. Sci. Technol. A **9**, 2477 (1991).
- <sup>14</sup>A. F. Devonshire, Philos. Mag. **40**, 1040 (1949).
- <sup>15</sup>A. F. Devonshire, Philos. Mag. **42**, 1065 (1951).
- <sup>16</sup>A. F. Devonshire, Adv. Phys. **3**, 85 (1954).
- <sup>17</sup>M. E. Lines and A. M. Glass, *Principles and Applications of Ferroelectrics and Related Materials* (Clarendon, Oxford, 1977).
- <sup>18</sup>V. Sundar and R. E. Newnham, Ferroelectrics **135**, 431 (1992).
- <sup>19</sup>G. A. Smolenskii and K. I. Rozgachev, Zh. Tekh. Fiz. **24**, 1751 (1954).
- <sup>20</sup>K. A. Müller and H. Burkard, Phys. Rev. B **19**, 3593 (1979).
- <sup>21</sup>K. Uchino, S. Nomura, L. E. Cross, S. J. Jang, and R. E. Newnham, J. Appl. Phys. **51**, 1142 (1980).
- <sup>22</sup>T. Yamada, J. Appl. Phys. **43**, 328 (1972).
- <sup>23</sup>D. R. Lide, *Handbook of Chemistry and Physics*, 76th ed. (CRC, Boca Raton, FL, 1995).
- <sup>24</sup>Y. Yano, K. Iijima, Y. Daitoh, T. Terashima, Y. Bando, Y. Watanabe, H. Kasatani, and H. Terauchi, J. Appl. Phys. **76**, 7833 (1994).
- <sup>25</sup>T. Shimizu, Solid State Commun. **102**, 523 (1997).
- <sup>26</sup>C. M. Cotell, J. S. Horwitz, J. A. Sprague, R. C. Y. Auyeung, P. D. Antonio, and J. Konnert, Mater. Sci. Eng., B **32**, 221 (1995).
- <sup>27</sup>L. Ryen and E. Olsson, J. Appl. Phys. **83**, 4884 (1998).